This is a repository copy of *Low-complexity UAC modem and data packet structure*.

White Rose Research Online URL for this paper:
https://eprints.whiterose.ac.uk/133141/

Version: Accepted Version

Low-Complexity UAC Modem and Data Packet Structure

Y. Zakharov[†], Y. Fei[‡], P. Mitchell[†], N. Morozs[†], B. Henson[†], L. Shen[†], T. Tozer[†]

[†]Department of Electronic Engineering, University of York, UK
[‡]Key Laboratory of Underwater Acoustic Communication & Marine Information Technology,
Communication Engineering Department of Xiamen University (China)

Abstract—In underwater acoustic communication (UAC), the propagated signal undergoes severe multipath and Doppler distortions. The high overall complexity of UAC receivers is essentially due the Doppler estimation, channel estimation and equalization techniques required to deal with these effects. In this paper, we propose a novel data packet structure for transmission in underwater acoustic channels. This data structure allows the development of relatively simple estimation and equalization techniques, thus resulting in a low-complexity modem design. The data packet is based on single-carrier modulation with superimposed data and pilot symbols. The pilot symbol sequence is repeated within the packet, thus allowing application of the multi-branch autocorrelation Doppler estimation, possessing a low complexity and high accuracy. The data rate in the packet can easily be adjusted depending on the propagation conditions. The received packet is processed in the frequency domain, thus allowing low-complexity channel estimation and equalization. More specifically, in the example design, the channel estimation is based on local cubic B-splines. The modem has been evaluated using numerical simulation and experiments in a water tank, demonstrating successful performance of our design.

I. INTRODUCTION

In underwater acoustic communication (UAC), the propagated signal undergoes severe multipath and Doppler distortions. The high overall complexity of UAC receivers is essentially due to the complexity of Doppler estimation, channel estimation and equalization techniques. Modems with multi-carrier modulation, such as Orthogonal Frequency Division Multiplexing (OFDM) [1]–[4], exhibit good performance and relatively low complexity of channel estimation and equalization as most of the signal processing is performed in the frequency domain. However, OFDM signals have a high peak to average power ratio (PAPR), which places severe demands on the power amplifier at the transmitter. OFDM signals are also sensitive to Doppler distortions in the channel, thus requiring complicated Doppler estimators. Single-carrier transmission on the other hand has lower PAPR and is less sensitive to the Doppler effect. There are many good schemes proposed for single-carrier transmission in underwater acoustic (UWA) channels, e.g. see [5]–[8]. They are typically designed for specific applications, with specific data rates, pilot structure, etc. We would like to propose for consideration a universal data packet structure, which is flexible in data rate and data packet length, while allowing relatively simple receivers.

The proposed scheme uses single-carrier modulation. It permits use of packets of variable length and with a large variety of data rates. The receiver in the modem detects the data packet, finds the temporal centre of the packet and performs initial estimation of Doppler parameters, such as the linear and quadratic time compression factors. Such a model of the Doppler effect allows communication in scenarios with transmitter/receiver motion at high velocity and acceleration [9]. This processing is performed independently (blindly) of the specific pilot sequence incorporated into the data packet. The data and pilot sequences are superimposed. The rest of the processing, including the re-sampling, channel estimation, equalization, fine Doppler estimation and correction, symbol demodulation and diversity combining, are performed in a turbo-iterative manner. In this version of the modem, data decoding is outside the turbo iterations; however, it can also be incorporated into the turbo-loop. The complicated parts of the receiver such as the channel estimation and equalization are performed in the frequency domain to reduce the receiver complexity.

One of most accurate methods of Doppler estimation in UWA multipath channels is based on computing the cross-ambiguity function (CAF) between received and transmitted signals [10]–[13]. The CAF is computed on a two-dimensional (2D) grid of channel delays and Doppler compression factors. The position of the maximum CAF magnitude over the Doppler grid provides an estimate of the Doppler compression due to the transmitter/receiver velocity. However, due to a large number of potential Doppler estimation channels, the CAF method is computationally intensive, even if fast Fourier transforms (FFTs) and a two-step (coarse and fine estimation) approach are used to speed up the computations [4], [14], [15]. In [9], [16], we have proposed a Doppler estimator that provides accurate estimates of Doppler compression factors due to the transmitter/receiver velocity and acceleration that requires significantly fewer computations than the CAF method. The design proposed in this paper is based on the Doppler estimator from [9], [16].

II. STRUCTURE OF THE TRANSMITTED DATA PACKET

The data packet is based on single-carrier modulation and superimposed pilot and data symbols. Its structure is shown in Fig. 1. The transmitted signal of duration Θ is given by
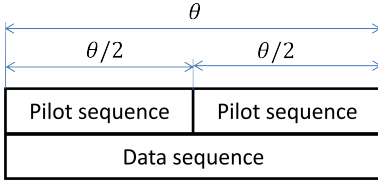
$$s(t) = s_d(t) + p(t) + p(t - \Theta/2), \qquad (1)$$
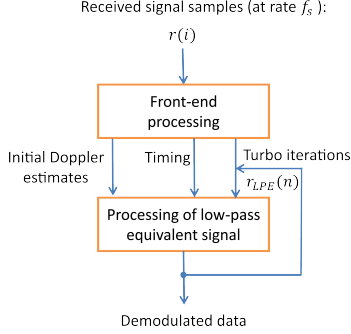
Fig. 1. Structure of the data packet.

Fig. 2. Structure of the receiver.

Fig. 3. Front-end processing in the receiver.

where $s_d(t)$ is the data signal of duration Θ carrying the data symbols, and $p(t)$ is the pilot signal of duration $\Theta/2$ carrying the pilot symbols.

In the example design, we use: (i) $\Theta = 1$ s; (ii) the pilot signal is pseudo-noise BPSK-modulated; (iii) the data symbols are BPSK modulated; (iv) the carrier frequency $f_c = 24$ kHz; (v) the symbol rate $F_d = 6 \times 10^3$ symbols/s, thus the data rate is 6 kbps; (vi) Root-Raised Cosine (RRC) pulse-shaping with the roll-off factor $\alpha = 0.2$. We combine BPSK data and pilot symbols to arrive at a combined QPSK symbol with the real and imaginary parts given by the pilot and data symbols, respectively. Note that other data signals, even multi-carrier data signals, can be used with such a structure.

III. DESCRIPTION OF THE MODEM

The receiver of the modem consists of two stages as shown in Fig. 2. The first stage, the front-end processing, works at a high sampling rate f_s (we use $f_s = 4f_c$) followed by a lower sampling rate F_s (we use $F_s = 2F_d$). The second stage, the low-pass equivalent (LPE) processing, includes a number of turbo-iterations performed at the symbol rate F_d.

A. Complex demodulation and RRC filtering

The input signal in the receiver is represented by real-valued samples $r(i)$ taken with a sampling interval $T_s = 1/f_s$. The front-end processing (see Fig. 3) includes complex demodulation consisting of multiplying the received signal by the complex exponential $e^{-j2\pi f_c i T_s}$ corresponding to the carrier frequency f_c, and the RRC filtering followed by the downsampling. In practice, the RRC filtering and downsampling are combined to reduce the complexity. Typically, the downsampling factor (8 in our design) is set to provide an oversampling factor of 2 with respect to the symbol rate F_d: $F_s = 2F_d$. The downsampled signal is treated as the LPE signal $r_{\mathrm{LPE}}(n)$ in the further processing.
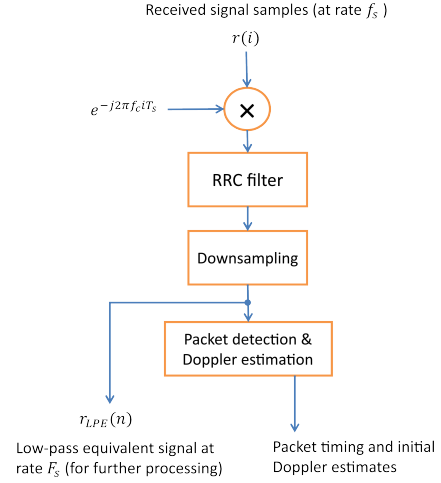
This processing in our realization requires 1.9×10^6 real-valued MAC (multiply/accumulate) [17], [18] operations per second. This takes into account that the RRC filter has 161 taps and there are F_s samples to be produced per second. This also takes into account the specific ratio $f_s = 4f_c$, for which the complex exponential contains 50% zeros and the remaining values are ± 1. Note that typical low-power DSP processors can provide 200×10^6 MACs, e.g., see [19]. This stage, if needed, can be comfortably implemented on an FPGA platform.

B. Data packet detection and Doppler estimation

The front-end processing (see Fig. 3) also includes the packet detection, timing estimation and initial Doppler estimation applied to the LPE signal $r_{\mathrm{LPE}}(n)$. These operations are based on the multi-branch autocorrelation Doppler estimator as described in our recent work [9].

For every sample $r_{\mathrm{LPE}}(n)$, the 2D autocorrelation function is computed as explained in [9]; an example is shown in Fig. 4. The maximum of the autocorrelation is shifted in delay and frequency with respect to the center of the delay-frequency plane. The delay and frequency shifts are proportional to the velocity v and acceleration a between the transmitter and receiver. The center corresponds to no time compression in the velocity (delay axis) and acceleration (frequency axis). The peak extracted from the autocorrelation function, as shown in Fig. 4, is further interpolated to improve the accuracy of estimation of the signal time compression in the channel.

The autocorrelation function in Fig. 4 corresponds to the maximum of the curve shown in Fig. 5. This curve is obtained by finding, for every sample at rate F_s, the maximum of the 2D autocorrelation function. The maximum in Fig. 5 is treated as an estimate of the temporal center of the data packet, where the second pilot sequence starts (see Fig. 1).

This computation, for our example design, requires about 29.6×10^6 MACs/s. This allows computation of 280 2D auto-correlation values to cover the velocity range $v \in [-5, 5]$ m/s
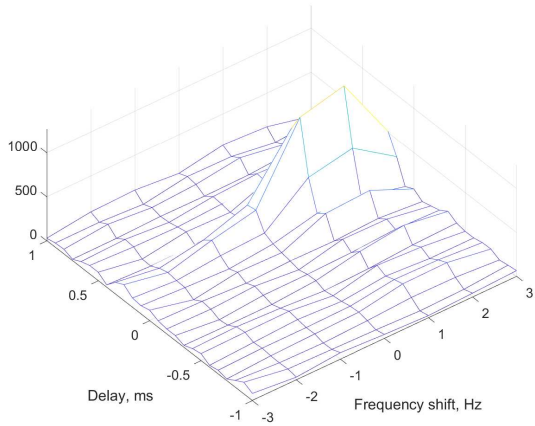
Fig. 4. 2D autocorrelation in a multipath channel with $v = 1$ m/s and $a = 0.2$ m/s^2 at the moment 1.5 s corresponding to the maximum in Fig. 5; SNR = 20 dB.
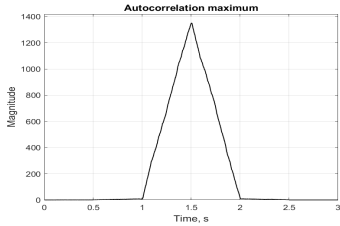

Fig. 5. Maximum of the autocorrelation as a function of time; SNR = 20 dB.

and acceleration range $a \in [-0.25, 0.25]$ m/s^2. This processing, if needed, can also be comfortably implemented on an FPGA platform.

C. Processing of the LPE signal

The LPE signal $r_{\text{LPE}}(n)$, initial Doppler parameters and the estimate of the temporal center (timing) of the data packet, obtained at the front-end processing stage, are then used at the LPE processing stage as shown in Fig. 6.

The processing is performed in a loop of N_{it} turbo iterations. Fig. 6 shows the processing in a single iteration and the feedback information used at the next iteration. The input signal $r_{\text{LPE}}(n)$ is resampled according to estimates of the Doppler parameters. At the first iteration, the initial Doppler estimates obtained at the front-end processing stage are used. At further iterations, fine Doppler estimates obtained in the previous turbo iteration are used. There are two branches of processing. Assuming that $F_s = 2F_d$, even samples of $r_{\text{LPE}}(n)$ are processed in the 'left' branch and the odd samples in the 'right' branch. The two branches perform the same processing. Therefore, we will describe here only one branch.

Channel estimation and equalization are done in the frequency domain. Transforming the single-carrier signal to the frequency domain simplifies the signal processing. The signal is transformed into the frequency domain using the FFT. The time window for the FFT is chosen based on the timing
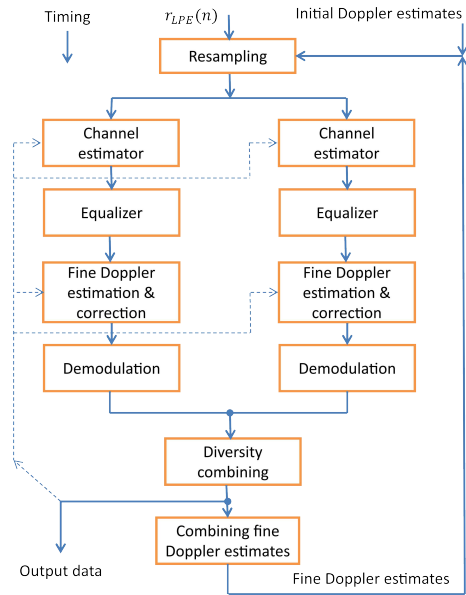

Fig. 6. Low-pass equivalent (LPE) processing in the receiver.

information that indicates the center of the data packet. The FFT length N_{FFT} is chosen to cover the data packet with a margin before the start and after the end of the received packet. In our example design, we use $N_{\text{FFT}} = 8192$, which with the packet length of $\Theta F_d = 6000$ symbols creates the margins of $(8192 - 6000)/2 = 1096$ symbols, or 183 ms from each side; this is longer than typical channel delay spreads. For the channel estimation, the approach is based on the basis expansion model (BEM) [20]–[29]. More specifically, B-splines are used allowing simple implementation. In particular, we use local B-splines, which possess especially low complexity [24]–[27]. The equalization is then performed in low-complexity subcarrier equalizers, similar to those in OFDM systems. The equalized signal is transformed back into the time domain using the inverse FFT (IFFT). At the first turbo iteration, the pilot symbols are used for the channel estimation, while at further iterations, both the pilot and tentatively demodulated data symbols are used for this purpose.

After the initial Doppler compensation, the residual Doppler distortion can be approximated as a linearly time-varying Doppler frequency. The fine Doppler estimation is based on the dichotomous frequency estimation [30], [31] and a similar dichotomous algorithm for fine estimation of linear-in-time dependence of the frequency. These are algorithms whose complexity is negligible compared to complexity of the other signal processing.

The fine Doppler estimates are used to provide an extra Doppler correction, which compensates for a residual Doppler effect still present in the processed signal and expressed as time compression due to the receiver/transmitter velocity and acceleration. The extra Doppler correction engenders an improvement in the detection performance. The two fine Doppler estimates obtained in the two branches are combined and used at the next turbo iteration for more accurate resampling.
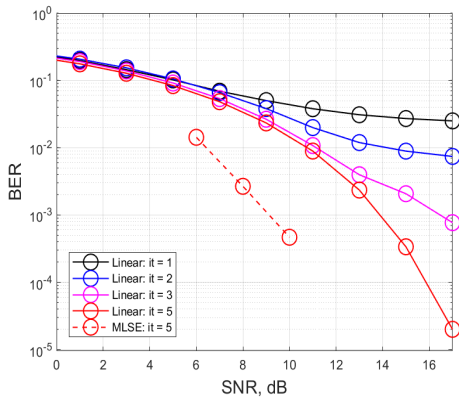
Fig. 7. Detection performance of the receiver *vs* turbo iteration (it $=$ $1, 2, 3, 5$) in the numerical simulation.

Fig. 8. Impulse response estimate obtained in the water tank experiment.

The Doppler compensated signals are demodulated according to the data constellation scheme used. The data estimates from the two branches are combined; in our example design, we use the maximal-ratio combining. The hard decision data estimates are then used at the next turbo iteration to improve channel and Doppler estimates.

The LPE processing has the following complexity. Assuming that a single FFT requires $4N_{FFT} \log_2 N_{FFT}$ real MACs, and there are 3 FFTs (one of the FFTs is applied to the pilot signal or pilot and data signal, and two others are applied to the received signal in two branches) and 2 IFFTs in every turbo iteration, we arrive for our example design with $N_{it} = 5$ turbo iterations at 10.6×10^6 MACs/s for all FFTs and IFFTs. Note that FFT is a standard operation for the FPGA design. The channel estimation based on the local cubic B-splines, for our case, requires about 1.3×10^6 MACs/s in 5 turbo iterations. The complexity of the other processing, including the equalization, Doppler fine estimation/correction, demodulation, etc., is negligible compared with the above. Resampling can be based on the local cubic splines [24], and its complexity is also small compared to the complexity of the other signal processing. Thus, the complexity in the turbo iterations is mainly due to the FFT/IFFT operations.

IV. NUMERICAL RESULTS

This section presents initial results obtained from a numerical simulation and an experiment in a water tank.

In the numerical simulation, we consider a channel model that consists of a linear system representing a static multipath channel followed by a time Doppler compression that is defined by a velocity $v = 1$ m/s and acceleration $a = 0.2$ m/s^2. The channel power delay profile (PDP) is defined by delays $(f_s/F_s)[1, 11, 80, 91, 100]$ and uniform path variances. Fig. 7 shows the BER performance (solid lines) in this scenario when the signal processing described above is used. It can be seen that the proposed receiver successfully operates in this scenario. It can also be seen how the detection performance improves with the number of turbo iterations; after five iterations, the performance does not improve further. Note
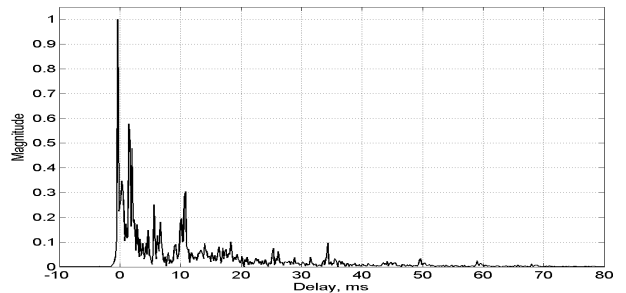
that if a higher-performance processor is available for the modem, more advanced signal processing can be employed in the receiver. As an example, Fig. 7 shows a performance of the receiver with an equalizer based on a box-constrained maximum-likelihood sequence estimation (MLSE). This processing would require about 400×10^6 MACs, but it provides an improved detection performance.

The water tank experiment was conducted in the University of Xiamen (China), in a tank of size 22.9 m $\times$ 5.2 m and maximum depth of 1.5 m. The distance between the transducer and receiver hydrophone was 18 m. Fig. 8 shows the impulse response measured by the receiver. All data packets have been detected and demodulated without errors with two turbo iterations. This experiment shows that the receiver can operate with real signals in a channel with a high delay spread.

We have also conducted air acoustic experiments in channels with high delay spreads and high Doppler effect. In these experiments, the data were also demodulated without errors.

V. CONCLUSIONS

We have proposed a signal structure for data packet transmission in UWA channels. This structure allows a low-complexity receiver implementation capable of dealing with the multipath propagation and the Doppler effect caused by the transmitter/receiver motion described by a velocity and acceleration. The Doppler estimator dominates the complexity of the receiver. The periodic structure of the pilot signal allows the use of the efficient multi-branch autocorrelation method. This method has significantly lower complexity compared to the Doppler estimator based on computing the ambiguity function and comparable accuracy [9]. The other signal processing in the receiver has lower complexity. Note that the proposed signal structure allows almost arbitrary data rates by choosing corresponding data modulation and coding. Importantly, the transmission with higher data rates is more sensitive to the channel and Doppler estimation. Our results show that for a data rate of 1 bps/Hz the proposed estimators provide a high detection performance.

REFERENCES

[1] B. Li, S. Zhou, M. Stojanovic, L. Freitag, and P. Willett, "Multicarrier communication over underwater acoustic channels with nonuniform Doppler shifts," *IEEE Journal of Oceanic Engineering*, vol. 33, no. 2, pp. 198–209, 2008.

[2] C. R. Berger, S. Zhou, J. C. Preisig, and P. Willett, "Sparse channel estimation for multicarrier underwater acoustic communication: From subspace methods to compressed sensing," *IEEE Transactions on Signal Processing*, vol. 58, no. 3, pp. 1708–1721, 2010.

[3] S. Yerramalli and U. Mitra, "Optimal resampling of OFDM signals for multiscale–multilag underwater acoustic channels," *IEEE Journal of Oceanic Engineering*, vol. 36, no. 1, pp. 126–138, 2011.

[4] Y. V. Zakharov and A. K. Morozov, "OFDM transmission without guard interval in fast-varying underwater acoustic channels," *IEEE Journal of Oceanic Engineering*, vol. 40, no. 1, pp. 144–158, 2015.

[5] M. Stojanovic, J. A. Catipovic, and J. G. Proakis, "Phase-coherent digital communications for underwater acoustic channels," *IEEE Journal of Oceanic Engineering*, vol. 19, no. 1, pp. 100–111, 1994.

[6] M. Johnson, L. Freitag, and M. Stojanovic, "Improved Doppler tracking and correction for underwater acoustic communications," in *IEEE Int. Conf. Acoustics, Speech, and Signal Processing, ICASSP-97*, 1997, vol. 1, pp. 575–578.

[7] T. J. Riedl and A. C. Singer, "Broadband Doppler compensation: Principles and new results," in *Conference Record of the Forty Fifth Asilomar Conference on Signals, Systems and Computers (ASILOMAR)*, 2011, pp. 944–946.

[8] K. A. Perrine, K. F. Nieman, T. L. Henderson, K. H. Lent, T. J. Brudner, and B. L. Evans, "Doppler estimation and correction for shallow underwater acoustic communications," in *2010 IEEE Conference Record of the Forty Fourth Asilomar Conference on Signals, Systems and Computers*, pp. 746–750.

[9] J. Li, Y. Zakharov, and B. Henson, "Multibranch autocorrelation method for Doppler estimation in underwater acoustic channel," *IEEE Journal of Oceanic Engineering, Early Access*, vol. 99, no. 1, pp. 1–1, 2017.

[10] G Jourdain, "Characterization of the Underwater Channel Application to Communication," in *Issues in Acoustic Signal-Image Processing and Recognition*, pp. 197–209. Springer, 1983.

[11] Y. V. Zakharov and V. P. Kodanev, "Experimental study of an underwater acoustic communication system with pseudonoise signals," *Journal of Acoustical Physics*, vol. 40, no. 9, pp. 707–715, 1994.

[12] Y. V. Zakharov and V. P. Kodanev, "Doppler scattering adaptive reception in a hydroacoustic communication channel," *Journal of Acoustical Physics*, vol. 41, no. 2, pp. 219–223, 1995.

[13] T. Arikan, T. Riedl, A. Singer, and J. Younce, "Comparison of OFDM and single-carrier schemes for Doppler tolerant acoustic communications," in *IEEE OCEANS-2015, Genova*, 2015, pp. 1–7.

[14] B. Li, S. Zhou, M. Stojanovic, L. Freitag, and P. Willett, "Non-uniform Doppler compensation for zero-padded OFDM over fast-varying underwater acoustic channels," in *IEEE OCEANS 2007-Europe*, pp. 1–6.

[15] S. F. Mason, C. R. Berger, S. Zhou, and P. Willett, "Detection, synchronization, and Doppler scale estimation with multicarrier waveforms in underwater acoustic communication," *IEEE Journal on Selected Areas in Communications*, vol. 26, no. 9, pp. 1638–1649, 2008.

[16] Y. V. Zakharov and J. Li, "Autocorrelation method for estimation of Doppler parameters in fast-varying underwater acoustic channels," in *Underwater Acoustics, Conference and Exhibition, UACE-2015. Crete, Greece.*, 2015, pp. 1–4.

[17] L. J. Karam, I. A. Kamal, A. Gatherer, G. Frantz, D. V. Anderson, B. L. Evans, et al., "Trends in multicore DSP platforms," *IEEE Signal Processing Magazine*, vol. 26, no. 6, pp. 38–49, 2009.

[18] A. Bateman and S. I. Paterson, *The DSP handbook*, Prentice-Hall, 2002.

[19] Texas Instruments, *TMS320C5545 Fixed-Point Digital Signal Processor*, 2016, http://www.ti.com/lit/ds/sprs853d/sprs853d.pdf.

[20] M. Visintin, "Karhunen-Loeve expansion of a fast Rayleigh fading process," *Electronics Letters*, vol. 32, no. 18, pp. 1712–1713, 1996.

[21] M. K. Tsatsanis and G. B. Giannakis, "Modelling and equalization of rapidly fading channels," *Int. J. Adaptive Contr. Signal Processing*, vol. 10, no. 2-3, pp. 159–176, 1996.

[22] Z. Tang and G. Leus, "Time-multiplexed training for time-selective channels," *IEEE Signal Processing Letters*, vol. 14, no. 9, pp. 585–588, 2007.

[23] G. Leus, "On the estimation of rapidly time-varying channels," *Proc. EUSIPCO'04, Vienna, Austria*, pp. 2227–2230, Sep. 2004.

[24] Y. V. Zakharov, T. C. Tozer, and J. F. Adlard, "Polynomial spline-approximation of Clarke's model," *IEEE Transactions on Signal Processing*, vol. 52, no. 5, pp. 1198–1208, 2004.

[25] Y. V. Zakharov, V. M. Baronkin, and J. Zhang, "Optimal and mismatched detection of QAM signals in fast fading channels with imperfect channel estimation," *IEEE Transactions on Wireless Communications*, vol. 8, no. 2, pp. 617–621, 2009.

[26] H. Mai, Y. V. Zakharov, and A. G. Burr, "Iterative channel estimation based on B-splines for fast flat fading channels," *IEEE Transactions on Wireless Communications*, vol. 6, no. 4, pp. 1224–1229, Apr. 2007.

[27] Y. V. Zakharov and T. C. Tozer, "Local spline approximation of time-varying channel model," *Electronics Letters*, vol. 37, no. 23, pp. 1408–1409, 2001.

[28] T. Zemen and C. F. Mecklenbrauker, "Time-variant channel estimation using discrete prolate spheroidal sequences," *IEEE Transactions on Signal Processing*, vol. 53, no. 9, pp. 3597–3607, 2005.

[29] P. S. Rossi and R. R. Muller, "Slepian-based two-dimensional estimation of time-frequency variant MIMO-OFDM channels," *IEEE Signal Processing Letters*, vol. 15, pp. 21–24, 2008.

[30] Y. Zakharov and T. Tozer, "Frequency estimator with dichotomous search of periodogram peak," *Electronics Letters*, vol. 35, no. 19, pp. 1608–1609, 1999.

[31] Y. Zakharov, V. Baronkin, and T. Tozer, "DFT-based frequency estimators with narrow acquisition range," *IEE Proceedings-Communications*, vol. 148, no. 1, pp. 1–7, 2001.